Turkish Journal of FISHERIES and AQUATIC SCIENCES

RESEARCH PAPER

Starvation Causes Energy Metabolism Alterations with The Stress and Immune Response Enhancement in *Parabotia fasciata*

Futie Zhang[1,2,3,*] , Xigeng Hu[1,2], Yunwen Cui[1,3], Tao Wang[1,2]

[1]Key Laboratory of Aquatic Biodiversity and Conservation of Chinese Academy of Sciences, Institute of Hydrobiology, Chinese Academy of Sciences, Wuhan 430072, China
[2]College of Fisheries and Life Science, Dalian Ocean University, Dalian, Liaoning Province 116023, China
[3]University of Chinese Academy of Sciences, Beijing 100049, China

How to Cite

Abstract

Fish often face starvation stress in the natural environment. *Parabotia fasciata* is widely distributed in China and very promising to become a new type of farmed fish. To understand the response mechanism of *P. fasciata* to starvation stress and to develop an economical and scientific feeding strategy, transcriptomic analysis was conducted in *P. fasciata* intestine in three experimental groups: satiated, semi-satiated and hungry. In the case of starvation, this fish reduced its metabolic levels. Immune and stress responses of *P. fasciata* were enhanced. And genes related to ubiquitination modification pathway, autophagy and lysosomal degradation pathway were also significantly upregulated. However, under starvation conditions, genes related to normally functional protein (amino acid) and fatty acid metabolism were down-regulated, genes related to glycogen synthesis pathway increased rapidly (glycogen synthase), while gluconeogenesis levels were slightly down-regulated, but genes related to glycogen hydrolysis and the glycolysis pathway were bidirectionally functioned. It suggests that protein and carbohydrate, instead of the fatty acid, maybe be the first choice of *P. fasciata* energy source in the case of starvation. This study provided valuable information for the metabolism and immune response in *P. fasciata* intestine under starvation conditions.

Introduction

Parabotia fasciata is widely distributed in the Heilongjiang River, Yellow River, Yangtze River and Pearl River of China, but has low natural yields. It has high protein content, rich in various essential amino acids, low fat content, while abundant in EPA (eicosapentaenoic acid) and DHA (docosahexaenoic acid), so it is highly nutritional and is favored by diners in Chongqing, Sichuan Provinces of China, with a high price in the market (Wu et al., 2011). At present, this fish is very promising to become a new type of farmed fish to meet people's demand for high-quality animal protein.

With the natural impacts of global climate change, predation and competition, as well as human interference such as overfishing, water conservancy projects, alien species invasion, and water

eutrophication, the wild resources of *P. fasciata* have been significantly reduced. The establishment of artificial breeding populations and the creation of new breeding strains are of great significance to the protection and rational utilization of its wild resources. At present, studies on the domestication and breeding of *P. fasciata* have been carried out, but the detailed feeding strategy is still blank. It is necessary to understand the response mechanism of *P. fasciata* to starvation stress and to develop an economical and scientific feeding strategy.

In the natural environment, fish often face starvation stress due to factors such as climate change, seasonal change, spatial distribution of food, competitive pressure and predator pressure. The physiological and biochemical changes of fish caused by starvation may affect the feeding behavior, growth and development, reproduction and immune response of

fish. Thus, fish, like other animals, have developed effective adaptive mechanisms to tolerate starvation in order to stabilize body structure and function (Secor & Carey, 2016). Bony fish belong to the lower vertebrates, unlike mammals, they do not need to expend extra energy to maintain body temperature, and can tolerate hunger for a long time under special circumstances (such as spawning, migration, food scarcity, etc.), so the adaptation mechanism of fish to hunger is more complex.

When hungry, animals usually use their body's stored energy to maintain normal metabolism and vital activities. Studies have shown that fish mainly consume two substances, fatty acid and carbohydrate, in the state of starvation (Jobling, 1980; Kutty, 1978; Poplawski et al., 2010). However, other studies have shown that when fish face starvation stress, they are more inclined to preferentially use lipids and proteins for energy supply (Lu et al., 2019).

Hung et al. (1997) found that lipids were the primary energy supply substances during starvation in *Acipenser transmontanus*. However, *Pagrus major* juvenile showed that fatty acid was not its primary energy substance (Kaneko, 2016). The liver glycogen of *Pelteobagrus fulvidraco* juvenile decreased significantly with the increase of fasting time (P<0.05), and quickly reached or was even significantly higher than that of the control group after 2 days of refeeding, indicating that glycogen is the first energy substance used by *P. fulvidraco* juvenile at the beginning of fasting (Li et al., 2014). Transcriptome analysis of large yellow croaker under starvation stress showed that starvation would cause significant expression of metabolism of energy substances such as body fat and protein and genes related to hormone synthesis in fish to resist stress damage (Qian et al., 2016). But the transcriptome data from the liver of starving zebrafish showed that there were significant changes in the pathways related to liver lipid metabolism (Xu et al., 2021). It can be seen that different fish choose different energy-supplying substances when they are hungry, and the physiological and biochemical response mechanisms are also different.

Global aquaculture production has expanded significantly in recent years, driven by improved farming techniques. To ensure sustainable growth, monitoring fish health through tissue analysis and biochemical parameters is critical (Faggio et al., 2014; Fazio et al., 2015). In this study, by comparing and analyzing the differences in the growth indicators and molecular responses of fish in full feeding, half feeding and starvation situations, the mechanism of response to hunger stress was analyzed, which provided references for the formulation of precise feeding strategies in domestication and species protection of *P. fasciata* in the future, and also had important theoretical and practical significance for the health management and sustainable development of the famous fish farming industry.

Materials and Methods

The Experiment Fish and Rearing Conditions

The experiment was carried out in indoor plastic breeding tanks (volume: 50 cm×40 cm×40 cm), which was connected with an oxygenating equipment and was continuously inflated every day. The water temperature, quality and fish health of each tank were monitored. During the experiment, water temperature ranged from 14℃ to 19℃, PH was about 8.2, dissolved oxygen ≥7.0 mg/L, ammonia nitrogen <0.2 mg/L, nitrite < 0.01 mg/L.

The experimental fish were 15-month-old *P. fasciata* artificially bred by our team. After fasting for 24h, individuals with healthy physique and uniform sizes were randomly placed into 3 experimental boxes, with 26 fish per box and average weight of (1.53±0.27) g.

Feeding and Management

Forage with a particle size of 1 mm (crude protein 36% and crude fat 8%) was set up in three experimental groups: satiated, semi-satiated and hungry (corresponding to groups A, B and C, respectively). Group A was fed normally, that is, feeding at 8:00 and 20:00 every day, with 4% of the total mass of the fish in the tank. Group B was fed at 20:00 every day, with 2% of the fish body mass. Group C was not fed during the whole experiment. Before the experiment, the experimental fish were domesticated for 3 days (3 d) and fed normally. Remove bait, feces and other dirt at 19:00 every day, and change the water with 1/3 amount in each tank once every two days.

Sampling

Anesthesia was administered to the fish with 20mg/L of MS-222. Sampling commenced once the fish exhibited loss of equilibrium. At the beginning of the experiment (0 d), 2 fish were randomly sampled from each group. On the 3d, 9d and 15 d, 6 fish were randomly sampled from each breeding box. The full length and body length of the fish were measured with vernier calipers, and the body mass after moisture absorption was measured with electronic balance. Then the fish was dissected and the intestinal filling and empty shell quality were recorded. Foregut tissues were taken, washed with sterile, enzyme-free water and cut into pieces, then put into a frozen storage tube filled with RNA preservation solution, and transferred to the freezer at -80℃ for subsequent RNA extraction and transcriptome analysis.

The intestinal tissues were used for the transcriptome sequencing. A total of 60 samples participated in sequencing. Due to the small size of the experimental fish and the insufficient amount of intestinal tissue samples, the intestinal tissues of two individuals treated in the same group at the same time were combined into one sample, thus totaling 30 samples. According to the different feeding frequency,

they were divided into 0 group (control group), A group (normal feeding), B group (half feeding) and C group (fasting). According to sampling time, group A was divided into A3 group (3 d), A9 group (9 d) and A15 group (15 d). Groups B and C were also ordered accordingly.

Biological Data Processing and Analysis

The weight gain rate (WGR) was calculated using the initial average body mass and the average body mass at the time of sampling. Condition factor (CF) was calculated based on body length and body mass data. The hepato-somatic index (HSI) and viscero-somatic index (VSI) are calculated based on the liver weight and shell weight measured by anatomic sampling. Relevant indicators are calculated as follows:

$$WGR\ (\%) = 100 \times (W_t - W_0)/W_0$$

$$CF\ (g/cm^3) = 100 \times W_t/L^3$$

$$HIS = 100 \times Liver\ Weight\ (g)/\ Body\ Weight\ (g)$$

$$VSI = 100 \times [Body\ Weight\ (g) - Shell\ Weight\ (g)]/\ Body\ Weight(g)$$

W_0 and W_t represent the initial body mass and the final body mass (g), t represents the feeding time (d), and L represents the body length (cm) of *P. fasciata*. The experimental data were analyzed using SPSS 22.0 and presented as "mean ± S.D". Kolmogorov-Smirnov and One-way ANOVA tests were used for the data proof. If there was any difference, Duncan's method was used for multiple comparisons between groups, and the significance level was set at $P < 0.05$.

RNA Extraction and Transcriptome Sequencing

Total RNA was extracted using a TRIzol Reagent Kit (Invitrogen, Life Technologies, MD). RNA degradation and contamination were monitored on 1% agarose gels. The purity, concentration and integrity of RNA samples were tested using NanoDrop 2000 and Agient2100/LabChip GX. A total amount of 1 μg RNA per sample was used as input material for the RNA sample preparations. Sequencing libraries were generated using NEBNext®Ultra™ RNA Library Prep Kit for Illumina® (NEB, USA) following manufacturer's recommendations. Then the library fragments were purified with AMPure XP system (Beckman Coulter, Beverly, USA). 3 μl USER Enzyme (NEB, USA) was used with size-selected, adaptor-ligated cDNA at 37°C for 15 min followed by 5 min at 95°C before PCR. Then PCR was performed with Phusion High-Fidelity DNA polymerase, Universal PCR primers and Index (X) Primer. At last, PCR products were purified (AMPure XP system) and library quality was assessed on the Agilent Bioanalyzer 2100 system. The clustering of the index-coded samples was performed on a cBot Cluster Generation System using TruSeq PE Cluster Kit v3-cBot-HS (Illumia) according to the

manufacturer's instructions. After cluster generation, the library preparations were sequenced on a sequencing platform and paired-end reads were generated. The sequences were further processed with a bioinformatic pipeline tool, BMKCloud (www.biocloud.net) online platform. Raw data (raw reads) of fastq format were firstly processed through in-house perl scripts. At the same time, Q20, Q30, GC-content and sequence duplication level of the clean data were calculated. All the downstream analyses were based on clean data with high quality.

Transcriptome Assembly and Gene Functional Annotation

Transcriptome assembly was accomplished using Trinity (Grabherr et al., 2011) with min_kmer_cov set to 2 by default and all other parameters set default. Gene function was annotated based on the following databases: NR (NCBI non-redundant protein sequences), Pfam (Protein family), KOG/COG/eggNOG (Clusters of Orthologous Groups of proteins), Swiss-Prot (A manually annotated and reviewed protein sequence database), KEGG (Kyoto Encyclopedia of Genes and Genomes), GO (Gene Ontology).

Quantification of Gene Expression Levels and Differential Expression Analysis

Gene expression levels were estimated by RSEM (Li and Dewey, 2011) for each sample. Clean data were mapped back onto the assembled transcriptome. And readcount for each gene was obtained from the mapping results. There are three biological replicates in our study. Differential expression analysis of two conditions/groups was performed using the DESeq R package (1.10.1). DESeq provide statistical routines for determining differential expression in digital gene expression data using a model based on the negative binomial distribution. The resulting P values were adjusted using the Benjamini and Hochberg's approach for controlling the false discovery rate. Genes with an adjusted *P*-value <0.05 found by DESeq were assigned as differentially expressed. Gene Ontology (GO) enrichment analysis of the DEGs was implemented by the topGO R packages based on Kolmogorov–Smirnov test. KOBAS software was used to test the statistical enrichment of differential expression genes in KEGG pathways (https://www.genome.jp/kegg/).

Real-Time qPCR Verification of Typical DEGs

Total RNA was extracted from the 30 intestine samples in 0 group (control group), A group (normal feeding), B group (half feeding) and C group (fasting) using a reagent kit (Transgen, Beijing, China). The quality and concentration of RNA were assessed using a spectrophotometer (Nanodrop8000, Thermo, USA). Subsequently, 1 μg of total RNA was reverse transcribed

into cDNA using the cDNA Synthesis Kit (Transgen, Beijing, China). Quantitative real-time PCR (qPCR) was used to detect gene expression patterns with a quantitative PCR detection system (Bio-Rad, USA). Three reference genes (β-*actin*, *Gapdh*, and *18S rRNA*) (Chen et al., 2022) were screened and compared, and *18S rRNA* was found more stable than other reference genes. Thus, *18S rRNA* was used as an internal control. The relative expression levels were calculated using the $2^{-\Delta\Delta Ct}$ method (Livak & Schmittgen, 2001). The statistical analysis was performed using SPSS 16.0 software. The results are presented as mean ± standard error (SE). Independent sample t-tests or one-way analysis of variance (ANOVA) were used.

Results

Effects of Different Feeding Ways on Growth Performance of *P. fasciata*

The effects of the three feeding ways on the growth performance of *P. fasciata* after 15-day experiment were shown in Table 1. There was no significant difference in average initial mass among all groups (P>0.05) and the survival rate among all groups in this experiment was 100%. There were significant differences in CF, VSI and HSI (P<0.05), while there were moderate differences in FBW and WGR (P>0.05).

Transcriptome Sequencing and Assembly Results

A total of 616.55 M Reads were obtained from 30 intestinal samples of *P. fasciata* by Illumina, with a total of 184.21 Gb of Clean Data. The average data volume of the samples was 6.14 Gb, the percentage of Q30 base was no less than 85.01%, and the average GC content was 46.5%. After assembly, 64226 Unigenes were obtained, and the Unigene N50 was 3265, indicating high assembly integrity. The result statistics are shown in Table S1.

Unigene Function Annotation Distribution

The sequences of unigenes were blasted against databases including NR, Swiss-Prot, COG、KOG, eggNOG4.5, KEGG by DIAMOND (Buchfink et al., 2015). KEGG Orthology of unigenes were obtained by KOBAS (Xie et al., 2011). InterProScan (Jones et al., 2014) uses the InterPro integrated database to analyze the GO (Ashburner et al., 2000) Orthology results of novel genes. The amino acid sequences of unigenes were predicted and the predicted sequences were annotated by blasting against the Pfam (Finn et al., 2013) database by HMMER (Eddy, 1998). In this project, By electing BLAST parameters E-value that are not greater than 1e[-5] and HMMER the parameters E-value that are not greater than 1e[-10], a total of 32,581 annotated Unigenes were obtained.

The annotation results are shown in Table S2. Among them, 29,073 Unigenes were annotated to NR database (89.23%), 15, 105 Unigenes were annotated to SwissProt database (46.36%), and 6485 Unigenes were annotated to COG database (19.90%). 25,822 Unigenes were added to the GO database (79.43%), 18,867 Unigenes were added to the KOG database (57.90%), and 24,623 Unigenes were added to the KEGG database (75.57%). There were 24,568 Unigenes notes to the eggNOG database (75.41%), 22,656 Unigenes notes to the Pfam database (69.54%), and 29,402 Unigenes notes to the TrEMBL database (90.24%).

Differential Expression Analysis

(1) Volcano Map on DEGs

Volcano plots of two samples were shown below. In this experiment, C3 and C9 samples were taken as an example. Among the 18,316 genes referred to in this study, 3936 genes were expressed differently in these two samples, including 1705 up-regulated genes and 1869 down-regulated genes. As shown in Figure S1, each point in the differential expression volcano map represents a gene, and the horizontal coordinate represents the logarithmic value (significance) of the multiple difference of expression of a certain gene in the two samples. The ordinate represents the negative pair value of the error detection rate (the magnitude of the difference). The blue dots represent down-regulated DEGs, the red dots represent up-regulated DEGs, and the gray dots represent non-DEGs.

(2) Clustering of DEGs

To identify potential functions of genes with similar expression patterns based on genes with known functions. Taking C3 and C9 as an example (Figure S2), each column represents a different sample, each row represents a different gene, and the color represents how much the gene is expressed in the sample, with red representing up-regulated genes and blue representing down-regulated genes. The cluster map showed similar expression patterns of genes with similar functions, providing a theoretical basis for subsequent screening of functionally related or similar genes.

(3) Enrichment Analysis of DEGs

The DEGs identified in differential expression analysis were annotated. The summary of annotations was shown in the Table S3. Criteria for DEGs was set as Fold Change≥1.5 and Pvalue<0.01. As shown in the statistical histogram of DEGs (Figure 1), there were more DEGs between group 0 and group C (C3, C9 or C15), A3 and C3, C3 and C9 pairs than others, and the amount of DEG was more than 3000. The number of DEGs between groups A15 and B15 is fewest. Significant differences appeared between group 0 and Group C (C3, C9, C15),

Table 1. Impact of feeding ways on the growth performance of *P. fasciata*

Groups	A	B	C
Initial body weight IBW/ (g)	1.53±0.25	1.54±0.25	1.52±0.26
Final body weight FBW/(g)	1.55±0.23	1.54±0.26	1.46±0.27
Survival rate SR/ (%)	100	100	100
Weight gain rate WGR/ (%)	1.29±3.34	0.11±3.76	-3.82±4.00
Condition factor CF/(g/cm³)	0.0101±0.001[a]	0.0097±0.001[ab]	0.0094±0.001[b]
Viscero-somatic index VSI/ (%)	13.53±1.84[a]	12.67±2.57[ab]	11.20±2.50[b]
Hepato-somatic index HSI/ (%)	1.59±0.65[a]	1.38±0.42[ab]	1.13±0.33[b]
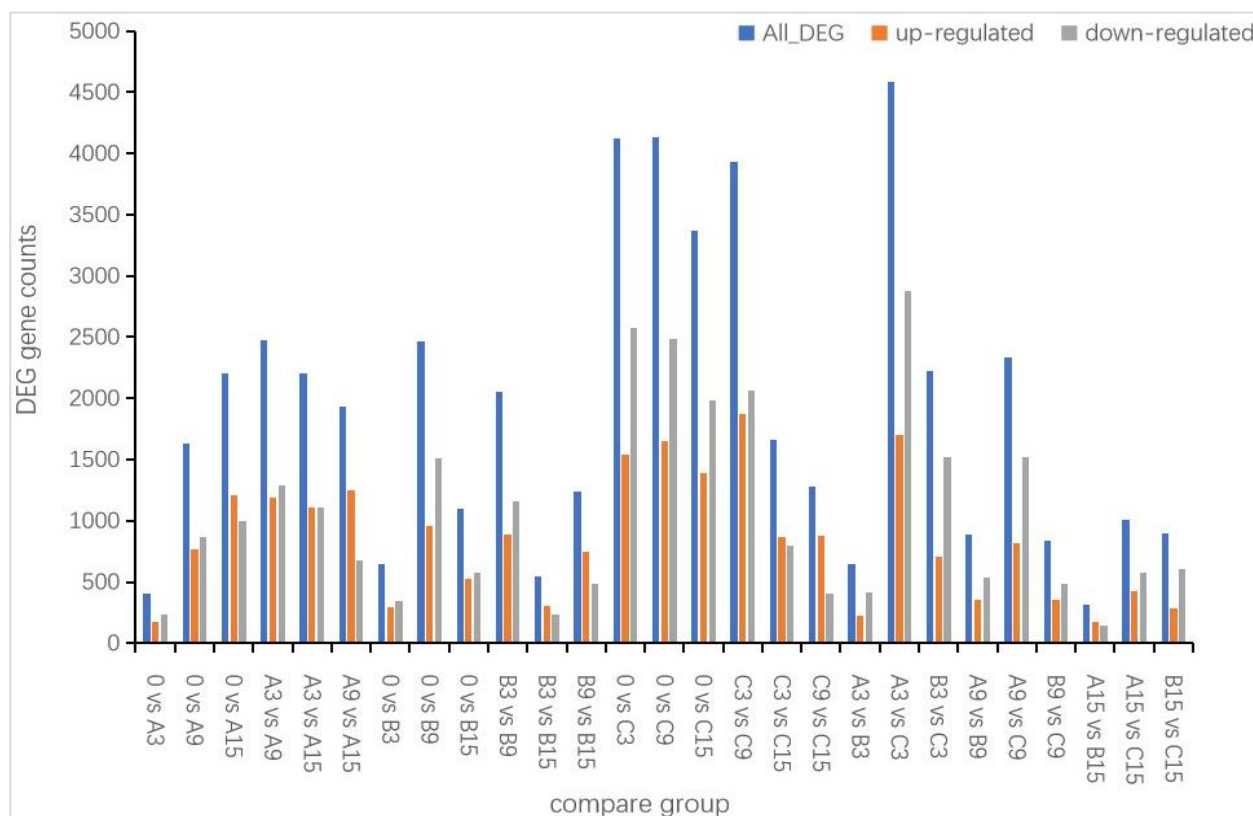
Figure 1. Bar chart of DEG statistics.

and also between groups A and C. Nearly all groups were dominated by down-regulated genes. It was obvious that *P. fasciata* reduced the level of its metabolic rate under the starvation condition (A to C) or suffered the deficient food awkward situation (A to B).

KGGG Enrichment Analysis

Pathway significance enrichment analysis took the pathway in KEGG database as the unit and applied hypergeometric test to find out the pathway of significant enrichment in DEGs compared with the whole genome background. Significant enrichment of pathway can identify the most important biochemical and metabolic pathways and signal transduction pathways involved in genes. ClusterProfiler was used to visualize the enrichment results using bubble graphs, bar graphs and network graphs. Taking group 0 and C15 samples as an example, the annotation results of DEGs were classified according to the pathway types in KEGG, and Figure 2 showed the top 20 pathways with the

lowest significant qvalue. It can be found that in the process of starvation stress, the number and proportion of DEGs annotated by endocytosis, carbon metabolism, protein processing in the endoplasmic reticulum, MAPK signaling pathway and PPAR signaling pathway were abundant, as shown in Figure S3. As is shown in Figure 2, the qvalues of fatty acid metabolism, primary bile acid biosynthesis, fatty acid degradation, PPAR signaling pathway, peroxisome, biosynthesis of unsaturated fatty acids, valine, leucine and isoleucine degradation, steroid hormone biosynthesis, carbon metabolism, tryptophan metabolism and proteasome pathways were significant. Fatty acid metabolism, carbon metabolism, PPAR signaling pathway and other related genes are abundant. Among them, primary bile acid biosynthesis, fatty acid degradation, peroxisome and tryptophan metabolism were significantly down-regulated.

According to KEGG enrichment analysis, 21 differential genes among PPAR signaling pathway were screened, as shown in Table 2. TRINITY_DN1654_c1_g1 (fatty acid-binding protein 2), TRINITY_DN28332_c6_g1
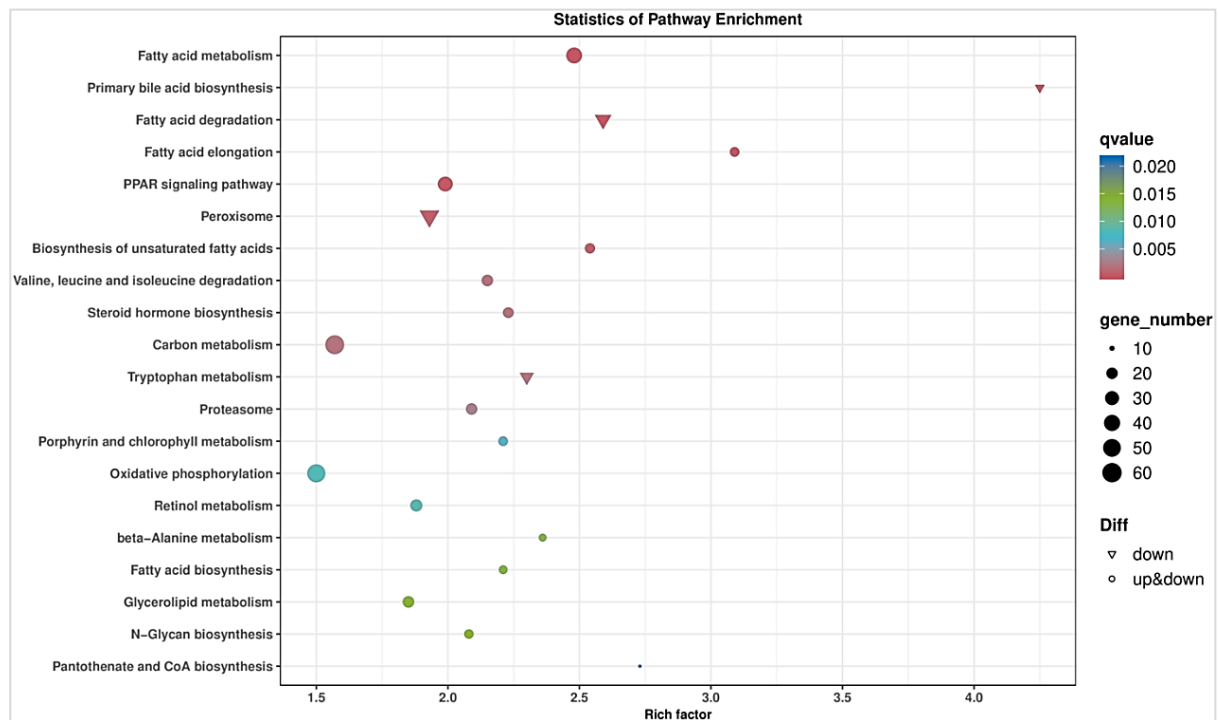
Figure 2. KEGG enrichment bubble chart for samples 0 and C15.

Note: Each circle in the figure represents a KEGG pathway, the ordinate represents the pathway name, and the abscess represents Enrichment Factor (Enrichment Factor), which represents the ratio of the proportion of differential genes annotated to a pathway to the proportion of all genes annotated to that pathway. The higher the enrichment factor, the more significant the enrichment level of DEGs in this pathway. The color of the circle represents qvalue, and the smaller the qvalue, the more reliable the enrichment significance of DEGs in this pathway. The size of the circle indicates the number of genes enriched in the pathway, and the larger the circle, the more genes. The closer to the path represented by the graph in the upper right corner of the diagram, the greater the reference value.

(apolipoprotein A-II), TRINITY_DN30626_c0_g1 (malate dehydrogenase), TRINITY_DN3435_c0_g1 (perilipin), and TRINITY_DN 47033_c0_g1 (Acyl-CoA desaturase), TRINITY_DN5725_c0_g1 (long-chain acyl-CoA ligase 5), TRINITY_DN8789_c0_g1 (fatty acid-binding protein 1) and other genes were related to peroxisome proliferator activation receptor (PPAR) signaling pathway, and most of them were down-regulated after starvation.

Innate immunological response of *P. fasciata* was enhanced by short-time fasting, such as TRINITY_DN37247_c0_g1 (tumor D54-like isoform X8), TRINITY_DN8387_c0_g1 (Glutaminyl-peptide cyclotransferase), TRINITY_DN4497_c0_g1 (fos-related antigen 1 –like isoform x1) and TRINITY_DN7334_c0_g1 (mannose-binding protein-like). And the expression of genes related to stress responses was strongly upregulated, such as TRINITY_DN17609_c0_g1 (hsp beta-11).

Under starvation conditions, the genes related to ubiquitination modification pathway, autophagy and lysosomal degradation pathway were significantly upregulated, such as TRINITY_DN9639_c0_g1 (Myotubularin-related protein 8, MTMR8), TRINITY_DN6724_c0_g2 (E3 ubiquitin-protein ligase), TRINITY_DN2892_c0_g1 (E3 ubiquitin-protein ligase SH3RF1) and TRINITY_DN86_c1_g1 (Autophagy-related protein 2), while TRINITY_DN9407_c0_g1 (Guanidinoacetate N-methyltransferase, GAMT) and TRINITY_DN8180_c0_g1 (serine protease 27) presented

a declining trend. It suggested that the misfolded or devitalized proteins were preferentially degraded, but the metabolism of properly functional protein such as muscle and normal protein hydrolysis and amino acid transport were weakened.

Under starvation conditions, DEGs related to fatty acid degradation pathway were conformably down-regulated, such as TRINITY_DN1620_c0_g1 (Acyl-coenzyme A oxidase), TRINITY_DN5725_c0_g1 (long-chain acyl-CoA ligase 5) and TRINITY_DN8229_c0_g1 (Non-specific lipid-transfer protein), which indicated the fatty acid was not the first choice of *P. fasciata* energy source in the case of starvation.

DEGs related to glycogen synthesis pathway increased slowly under starvation conditions (glycogen synthase, such as TRINITY_DN33103_c0_g1). The genes related to the glycogen hydrolysis pathway and the glycolysis pathway were up-regulated or down-regulated, while the levels of gluconeogenetic genes were slightly down-regulated.

Lipid, protein and carbohydrate are the three main energy resources of animals. The DEGs among fatty acid metabolism pathway were decreased after starvation, but DEGs from protein and carbohydrate metabolism pathways were more complicated in this study, both increasing and declining statuses presented, so it can be deduced that protein and carbohydrate, instead of fatty acid, may be the primary energy choice of *P. fasciata* when encountering the starvation situation.

Table 2. Analysis of differential gene expression levels in KEGG

#ID	Gene name	Expression level									
		0	A3	A9	A15	B3	B9	B15	C3	C9	C15
PPAR signaling pathway											
TRINITY_DN15879_c1_g1	Medium-chain specific acyl-CoA dehydrogenase	1.00	1.27	1.40	1.08	0.92	0.97	1.07	0.92	1.01	0.75
TRINITY_DN1620_c0_g1	Acyl-coenzyme A oxidase	1.00	1.21	0.68	0.56	0.75	0.33	0.61	0.35	0.30	0.25
TRINITY_DN1654_c1_g1	Fatty acid-binding protein 2	1.00	1.22	1.25	0.77	0.91	0.50	0.79	0.38	0.30	0.34
TRINITY_DN18503_c0_g1	Fatty acyl desaturase 2	1.00	1.26	1.15	0.51	0.79	0.64	0.50	0.48	0.55	0.43
TRINITY_DN24372_c0_g1	Fatty acid desaturase 2	1.00	1.52	1.17	0.53	0.96	0.69	0.69	0.69	0.61	0.55
TRINITY_DN27095_c0_g2	Fatty acyl desaturase 2	1.00	1.30	1.12	0.63	0.92	0.65	0.69	0.59	0.55	0.49
TRINITY_DN28332_c1_g1	Apolipoprotein A-II	1.00	1.98	1.46	0.49	0.87	0.19	0.59	0.30	0.00	0.03
TRINITY_DN28332_c6_g1	Apolipoprotein A-II	1.00	1.28	1.63	0.87	0.68	0.60	0.71	0.60	0.50	0.51
TRINITY_DN30626_c0_g1	Malate dehydrogenase	1.00	1.02	0.27	0.34	0.61	0.14	0.48	0.30	0.09	0.15
TRINITY_DN3435_c0_g1	Perilipin	1.00	0.82	3.69	0.70	0.21	1.70	0.50	0.22	0.74	0.93
TRINITY_DN37_c0_g3	Retinoic acid receptor RXR-alpha isoform X3	1.00	1.17	0.69	1.22	1.25	1.20	1.16	1.18	1.26	1.49
TRINITY_DN38580_c0_g1	Acetyl-CoA acetyltransferase A	1.00	1.29	1.29	0.94	0.93	0.75	1.01	0.60	0.71	0.58
TRINITY_DN42033_c0_g1	Fatty acyl desaturase 2	1.00	1.18	1.03	0.48	0.81	0.66	0.50	0.45	0.48	0.44
TRINITY_DN4427_c0_g1	Phosphoenolpyruvate carboxykinase	1.00	1.13	1.10	0.78	0.95	0.65	0.73	0.94	0.53	0.48
TRINITY_DN46107_c0_g1	Fatty acid binding protein 1	1.00	1.74	2.00	0.94	1.08	0.71	1.08	0.15	0.47	0.23
TRINITY_DN47033_c0_g1	Acyl-CoA desaturase	1.00	1.51	4.91	1.68	1.16	3.67	1.48	0.57	3.67	1.74
TRINITY_DN4705_c0_g1	AMP-binding domain-containing protein	1.00	1.40	1.43	0.75	1.06	0.89	0.83	0.52	0.83	0.72
TRINITY_DN5725_c0_g1	Long-chain-fatty-acid-CoA ligase 5	1.00	1.08	0.34	0.32	0.45	0.17	0.46	0.18	0.12	0.14
TRINITY_DN8229_c0_g1	Non-specific lipid-transfer protein	1.00	1.18	0.76	0.58	0.89	0.44	0.57	0.47	0.25	0.24
TRINITY_DN8668_c0_g1	FABP domain-containing protein	1.00	1.08	0.92	0.73	0.91	0.64	0.73	0.60	0.76	0.49
TRINITY_DN8789_c0_g1	Fatty acid binding protein 1	1.00	1.28	1.16	0.78	0.71	0.45	0.87	0.15	0.31	0.19
Stress and immune response											
TRINITY_DN17609_c0_g1	Hsp beta-11	1.00	2.73	8.99	13.10	3.43	9.54	10.20	4.30	25.20	21.91
TRINITY_DN4497_c0_g1	fos-related antigen 1-like isoform X1	1.00	0.29	0.62	1.00	0.71	2.69	0.64	0.50	1.25	34.89
TRINITY_DN37247_c0_g1	tumor D54-like isoform X8	1.00	0.63	1.64	2.77	1.35	2.23	2.64	1.54	2.70	5.10
TRINITY_DN7334_c0_g1	mannose-binding protein	1.00	1.37	1.82	3.81	2.19	3.15	3.83	2.28	3.41	6.05
TRINITY_DN8387_c1_g1	Glutaminyl-peptide cyclotransferase	1.00	0.89	0.73	0.92	1.32	1.19	1.10	1.91	1.21	0.77
Fatty acid degradation											
TRINITY_DN15879_c1_g1	Medium-chain specific acyl-CoA dehydrogenase	1.00	1.27	1.40	1.08	0.92	0.97	1.07	0.92	1.01	0.75
TRINITY_DN1620_c0_g1	Acyl-coenzyme A oxidase	1.00	1.21	0.68	0.56	0.75	0.33	0.61	0.35	0.30	0.25
TRINITY_DN18503_c0_g1	Fatty acyl desaturase 2	1.00	1.26	1.15	0.51	0.79	0.64	0.50	0.48	0.55	0.43
TRINITY_DN24372_c0_g1	Fatty acid desaturase 2	1.00	1.52	1.17	0.53	0.96	0.69	0.69	0.69	0.61	0.55
TRINITY_DN27095_c0_g2	Fatty acyl desaturase 2	1.00	1.30	1.12	0.63	0.92	0.65	0.69	0.59	0.55	0.49
TRINITY_DN38580_c0_g1	Acetyl-CoA acetyltransferase A	1.00	1.29	1.29	0.94	0.93	0.75	1.01	0.60	0.71	0.58
TRINITY_DN42033_c0_g1	Fatty acyl desaturase 2	1.00	1.18	1.03	0.48	0.81	0.66	0.50	0.45	0.48	0.44
TRINITY_DN47033_c0_g1	Acyl-CoA desaturase	1.00	1.51	4.91	1.68	1.16	3.67	1.48	0.57	3.67	1.74
TRINITY_DN4705_c0_g1	AMP-binding domain-containing protein	1.00	1.40	1.43	0.75	1.06	0.89	0.83	0.52	0.83	0.72
TRINITY_DN5725_c0_g1	Long-chain-fatty-acid--CoA ligase 5	1.00	1.08	0.34	0.32	0.45	0.17	0.46	0.18	0.12	0.14
TRINITY_DN8229_c0_g1	Non-specific lipid-transfer protein	1.00	1.18	0.76	0.58	0.89	0.44	0.57	0.47	0.25	0.24
Protein metabolism											
TRINITY_DN6724_c0_g2	E3 ubiquitin-protein ligase	1.00	0.42	0.40	0.81	0.54	0.95	0.88	0.72	0.68	6.79
TRINITY_DN86_c1_g1	Autophagy-related protein 2	1.00	0.97	0.95	1.25	1.61	1.32	1.31	2.14	1.28	1.52
TRINITY_DN2892_c0_g1	E3 ubiquitin-protein ligase SH3RF1	1.00	1.35	0.85	2.90	2.23	1.38	2.39	2.92	1.78	2.46
TRINITY_DN9639_c0_g1	Myotubularin-related protein 8	1.00	1.12	1.56	1.54	3.85	1.28	4.03	0.77	2.12	2.92
TRINITY_DN9407_c0_g1	Guanidinoacetate N-methyltransferase	1.00	0.98	0.65	0.48	0.84	0.34	0.49	0.57	0.30	0.18
TRINITY_DN8180_c0_g1	Serine protease 27	1.00	0.52	1.19	5.41	1.54	1.91	1.33	2.15	1.00	1.04
Glycogen hydrolysis											
TRINITY_DN772_c0_g1	Phosphorylase b kinase	1.00	0.97	1.37	1.94	1.43	1.28	2.48	2.63	1.94	2.47
TRINITY_DN1984_c0_g1	Phosphorylase b kinase	1.00	1.24	1.09	1.17	0.94	1.00	1.24	0.57	0.88	0.71
TRINITY_DN18927_c0_g1	Phosphoglucomutase	1.00	1.09	0.84	0.85	0.98	0.60	0.98	0.51	0.47	0.44
Glycogen synthesis											
TRINITY_DN33103_c0_g1	Glycogen synthase kinase-3	1.00	0.79	0.66	1.26	1.03	0.97	1.38	1.23	1.15	1.59
Glycolysis											
TRINITY_DN13608_c0_g1	Phosphotransferase	1.00	0.67	0.79	0.45	0.53	0.42	0.43	0.47	0.26	0.86
TRINITY_DN459_c1_g1	Hexokinase	1.00	0.94	0.83	0.68	0.67	0.59	0.79	0.38	0.41	0.36
TRINITY_DN499_c2_g1	Hexokinase	1.00	0.92	1.03	1.74	1.00	1.58	1.50	1.12	1.82	2.16
Gluconeogenesis											
TRINITY_DN2955_c0_g1	Phosphoenolpyruvate carboxykinase	1.00	0.08	0.60	0.67	0.67	0.91	0.52	0.44	0.47	0.62
TRINITY_DN4427_c0_g1	Phosphoenolpyruvate carboxykinase	1.00	1.13	1.10	0.78	0.95	0.65	0.73	0.94	0.53	0.48

When fish encounter the awkward situation of food shortage, the genes related to stress reaction and energy metabolism start to change correspondingly. When fish cannot get any food, these genes would be further regulated (Figure 1). Hence, most of DEGs in Table 2 showed a more dramatic change of the expression level in Group C than those in Group B.

The Results of Real-Time qPCR

With *18s rRNA* as inter-reference, nine genes linked to stress, immunity, protein and carbohydrate metabolism were randomly selected for qPCR validation. The primer sequence was the longest unigene by RNA-seq, and the internal reference sequence was the sequence of *Megalobrama amblycephala* which was downloaded from NCBI. The solubility curve of all unigenes was unimodal; therefore, the evidence showed that each of the products was singular. The overall consistency of gene expression from qPCR, and RNA-Seq (correlation coefficient of 0.67) revealed the sequence assembly and the expression analysis of genes provided reliable transcriptome information in this work (Figure S4).

Discussion

Food as a vital factor for the growth and survival of fish is capricious in the nature. Hence, fish developed differential adaptation mechanisms under deficient food states, especially starvation. This study indicated that protein and carbohydrate, instead of fatty acid, may be the primary energy choice of *P. fasciata* when encountering the starvation situation, which is different from the response of other fish (Jobling, 1980; Kutty, 1978; Li et al., 2014; Lu et al., 2019; Poplawski et al., 2010; Qian et al., 2016; Xu et al., 2021).

Peroxisome proliferator activated receptors (PPARs) play an important role in regulating lipid metabolism, adipocyte differentiation, and maintaining free fatty acid homeostasis in vivo, and are considered to be lipid metabolism receptors (Desvergne & Wahli, 1999). Nearly all DEGs in the PPAR signaling pathway and the fatty acid degradation pathway were decreased in hungry *P. fasciata* (Table 2), which obviously declaring the absence of fatty acid as a primary energy supply. But in large yellow croaker under starvation stress, significant expression of metabolism of energy substances such as body fat and protein and genes related to hormone synthesis were found (Qian et al., 2016). Significant changes were also discovered in the pathways related to lipid metabolism, including fatty acid metabolism, PPAR signaling pathway, fatty acid extension, fat digestion and absorption, and unsaturated fatty acid biosynthesis in the liver of starving zebrafish (Xu et al., 2021).

Phosphoenolpyruvate carboxykinase (PEPCK, TRINITY_DN2955_c0_g1 and TRINITY_DN4427_c0_g1) is the key enzyme of gluconeogenesis. Phosphoglucomutase (TRINITY_DN18927_c0_g1) and phosphorylase are the key enzymes of glycogen hydrolysis. Glycogen synthase (TRINITY_DN33103_c0_g1) is the key enzyme of glycogen synthesis. And phosphotransferase (TRINITY_DN13608_c0_g1) and hexokinase (TRINITY_DN459_c1_g1 and TRINITY_DN499_c2_g1) are the key enzymes of glycolysis. These DEGs presented a complicated alteration (increasing or decreasing) in this study (Table 2) under starvation period, suggesting a prior use of carbohydrate as an energy supply. Similarly, glycogen is the first energy substance used by *P. fulvidraco* juvenile at the beginning of fasting (Li et al., 2014). Both *P. fasciata* and *P. fulvidraco* choose carbohydrate (glycogen) as the first energy substance at the beginning of starvation, which would be related to the similar body shape (long cylindrical) and life habit (benthic and omnivorous), both significantly different from the counterpart traits of large yellow croaker (elongated and laterally flattened, benthic and carnivorous) and zebrafish (elongated and slightly fusiform, in lower-middle water and omnivorous).

Interestingly, *P. fasciata* presented a more complicated response, besides carbohydrate, the protein was also its primary energy source. Under the starvation stress, more proteins were misfunctioned or loss of ability than in normal states, and should be frequently renewed by protein degradation systems, i.e., the proteasome degrading ubiquitinated proteins, and cathepsins in lysosomes degrading exogenous proteins. The ubiquitin-proteasome system targets misfolded proteins for degradation. Since the accumulation of such proteins is potentially harmful for the cell, their prompt removal is important. E3 ubiquitin-protein ligases mediate substrate ubiquitination by bringing together the substrate with an E2 ubiquitin-conjugating enzyme, which transfers ubiquitin to the substrate. For misfolded proteins, substrate recognition is generally delegated to molecular chaperones that subsequently interact with specific E3 ligases (Boomsma et al., 2016). Autophagy also plays a critical role in nutrient recycling and stress adaptations (Rabinowitz & White, 2010), and autophagy-related protein 2 is a key molecular in the autophagy pathway (Hashimi et al., 2021). In this study, the expression of TRINITY_DN9639_c0_g1 (Myotubularin-related protein 8, MTMR8), TRINITY_DN6724_c0_g2 (E3 ubiquitin-protein ligase), TRINITY_DN2892_c0_g1 (E3 ubiquitin-protein ligase SH3RF1) and TRINITY_DN86_c1_g1 (Autophagy-related protein 2) enhanced dramatically. And this is a reasonable but quite unpredictable point in *P. fasciata* responses comparing with in other fish.

This study revealed that *P. fasciata* reduced the level of its metabolic rate under the starvation condition (A to C) or suffered the deficient food awkward situation (A to B) (Figure 1, Table 2). For example, guanidinoacetate N-methyltransferase (GAMT) is an enzyme that functions to create creatine (Cr), a substance used in the body to transfer and contain energy in the form of phosphate (Ostojic & Jorga, 2023). The expression of TRINITY_DN9407_c0_g1 (GAMT) downregulated slightly when food became less (Group A to Group B) but dramatically decreased under shot-time starvation (A to C) (Table 2). Ashouri et al. (2013) revealed that Siberian sturgeon survived the starvation period by reducing basal metabolic rate and energy storage. The consistency of fish reaction on starvation stress indicated that fish would live as long as possible by reduce its energy consumption rate until it gets a food resupply.

Another unpredictable result was that the stress and immunological response of *P. fasciata* was abundantly enhanced by short-time fasting, such as TRINITY_DN17609_c0_g1 (hsp beta-11) and TRINITY_DN4497_c0_g1 (fos-related antigen 1 –like isoform x1), TRINITY_DN37247_c0_g1 (tumor D54-like isoform X8), TRINITY_DN8387_c0_g1 (Glutaminyl-peptide cyclotransferase) and TRINITY_DN7334_c0_g1 (mannose-binding protein-like). Transport of proteins and lipids from one membrane compartment to another is via intracellular vesicles. Tumor protein D54, a symbol molecule in stress responses, is involved in multiple membrane trafficking pathways: anterograde traffic, recycling, and Golgi integrity (Gabrielle et al., 2020).

Glutaminyl-peptide cyclotransferase (QPCT) catalyzes the posttranslational modification of an N-terminal glutamate of proteins to pyroglutamate. QPCT is a resistance factor in bacterial infection in the innate immunity (Wang et al., 2018). Mannose-binding protein (MBP), as a pattern recognition receptor, is widely found in both vertebrates and invertebrates and proposed to play an important role in first-line defense by binding to multiple ligands on the pathogen surface and initiating humoral or cellular immune responses (Jack & Turner, 2003). The activator protein 1 (AP-1) family is a group of structurally and functionally related JUN and FOS [c-FOS, FOSB, Fos-related antigen 1 (FRA1), and FRA2] transcription factors. AP-1 heterodimers are involved in a variety of biological processes including cell proliferation, differentiation, apoptosis, and inflammation. FRA1 is involved in regulating the inflammatory immune response (Moon et al., 2017). Heat shock proteins (HSPs) belong to the class of highly conserved proteins that are widely present in eukaryotic and prokaryotic cells (Park & Seo, 2015) and play a key role in maintaining the steady state of intracellular proteins under normal physiological and stress conditions. During the stress response, the massive induction of heat shock proteins can protect animals from damage (Morimoto et al., 1992). Thus, the expression of TRINITY_DN17609_c0_g1 (hsp beta-11) was upregulated significantly. This is quite different from the response of white sturgeon, in which hunger would cause the decrease of its heat shock protein expression (Han et al., 2012). Despite the shortage of energy supply, the starveling *P. fasciata* was still enhanced the stress and immune responses to support itself to avoid the invasion by pathogenic microorganisms and live as long as it can. Short-term fasting or dietary restriction can enhance the body's immunity in yeast, worms, rodents and primates (Fontana et al., 2010). Fasting or restricted diets can reduce levels of proinflammatory factors in the blood, induce the body to degrade unwanted or damaged immune cells, and stimulate hematopoietic stem cells to produce new immune cells to restart the immune system (Jordan et al., 2019). And now the fish presented the coincident result.

In fish aquaculture, farmers often adopt the way of fasting and refeeding to induce the compensatory growth of fish, in order to reduce labor and feed costs, and reduce the pollution of the farming environment (Mccue, 2010). In addition, starvation is adopted as management to reduce mortality in the presence of disease, or improve pre-harvest fish flesh quality (Lv et al., 2018). This fasting and refeeding strategy would undoubtably adopted in the future farming of *P. fasciata*. And a forage with high carbohydrate is strongly suggested to be used after the short-time fasting fish because of the lower price of carbohydrate than that of proteins.

Conclusion

This study was conducted to elucidate the molecular response mechanisms of *P. fasciata* to starvation stress, and indicated that protein and carbohydrate, instead of fatty acid, may be the primary energy choice of *P. fasciata* when encountering the starvation situation. Meanwhile, the stress and immune response of *P. fasciata* was abundantly enhanced by short-time fasting. These findings will facilitate the development of balanced feeding strategies to optimize both growth performance and health management in *P. fasciata* aquaculture.

Ethical Statement

This study has been approved by the Ethics Committee for Animal Experiments of the Institute of Hydrobiology, Chinese Academy of Sciences and followed the legal requirements or guidelines in China for the care and use of animals.

Funding Information

Author Contribution

First Author: Study conception and design, project administration, methodology, supervision, writing review and editing; Second Author: Experiment, data collection, visualization and writing-original draft; Third Author: qPCR experiment, writing-review and editing. Last Author: Fish breeding and management. All authors read and approved the final manuscript.

Conflict of Interest

The authors declare that the research was conducted in the absence of any commercial or financial relationships that could be construed as a potential conflict of interest.

Acknowledgements

References

Ashburner, M., Ball, C.A., Blake, J.A., Botstein, D., Butler, H., Cherry, J.M., Davis, A.P., Dolinski, K., Dwight, S.S., Eppig, J.T., Harris, M.A., Hill, D.P., Issel-Tarver, L., Kasarskis, A., Lewis, S., Matese, J.C., Richardson, J.E., Ringwald, M.,

Rubin, G.M., & Sherlock, G. (2000). Gene ontology: tool for the unification of biology. Nature Genetics, 25(1), 25-29. https:// doi.org/10.1038/75556

Ashouri, G., Yavari, V., Bahmani, M., Yazdan, M.A., Kazemi, R., Morshedi, V., & Fatollahi, M. (2013). The effect of short-term starvation on some physiological and morphological parameters in juvenile Siberian sturgeon, *Acipenser baerii* (*Actinopterygii: Acipenseriformes: Acipenseridae*). Acta Ichthyologica et Piscatoria, 43 (2), 144-149. https:// doi.org/10.3750/aip2013.43.2.07

Boomsma, W., Nielsen, S.V., Lindorff-Larsen, K., Hartmann-Petersen, R., & Ellgaard, L. (2016). Bioinformatics analysis identifies several intrinsically disordered human E3 ubiquitin-protein ligases. PeerJ, 4, e1725.

Buchfink, B., Xie, C., & Huson, D.H. (2015). Fast and sensitive protein alignment using DIAMOND. Nature Methods, 12, 59-60.

Chen, J., Liu, H., Gooneratne, R., Wang, Y., & Wang, W. (2022). Population genomics of *Megalobrama* provides insights into evolutionary history and dietary adaptation. Biology, 11(2), 186. https://doi.org/10.3390/biology-11020186

Desvergne, B., & Wahli, W. (1999). Peroxisome proliferator-activated receptors: nuclear control of metabolism. Endocrine Reviews, 20(5), 649-688.

Eddy, S.R. (1998). Profile hidden Markov models. Bioinformatics, 14 (9), 755-763.

Faggio, C., et al. (2014).Effect of three different anticoagulants and storage time on haematological parameters of *Mugil cephalus* (Linneaus, 1758). Turkish Journal of Fisheries and Aquatic Sciences, 14(3), 615-621.

Fazio, F., et al. (2015). Peripheral blood and head kidney haematopoietic tissue response to experimental blood loss in mullet (*Mugil cephalus*). Marine Biology Research, 11(2), 197-202.

Finn, R.D., Bateman, A., Clements, J., Coggill, P., Eberhardt, R.Y., ..., & Punta, M. (2013). Pfam: the protein families database. Nucleic Acids Research, 42, D222-230. https://doi.org/10.1093/nar/gkt1223

Fontana, L., Partridge, L., & Longo, V.D. (2010). Extending healthy life span--from yeast to humans. Science, 328(5976), 321-326.

Gabrielle, L., Penelope, J.L.B., Nicholas, I.C., Nicholas, J.C., & Stephen, J.R. (2020). Tumor protein D54 defines a new class of intracellular transport vesicles. Journal of Cell Biology, 219 (1), e201812044.

Grabherr, M.G., Haas, B.J., Yassour, M., Levin, J.Z., ..., & Regev, A. (2011). Full-length transcriptome assembly from RNA-Seq data without a reference genome. Nature Biotechnology, 29, 644-652. https://doi.org/10.1038/nbt.1883

Han, D., Huang, S.S.Y., Wang, W.F., Feng, D.F., & Hung, S.S.O. (2012). Starvation reduces the heat shock protein responses in the white sturgeon larvae. Environmental biology of fishes, 93 (3), 333-342. https://doi.org/10.1007/s10641-011-9918-8

Hashimi, S.M., Wu, N.N., Ran, J., & Liu, J.Z. (2021). Silencing *Autophagy-Related Gene 2* (*ATG2*) results in accelerated senescence and enhanced immunity in soybean. International Journal of Molecular Sciences, 22(21), 11749.

Hung, S.S.O., Liu, W., Li, H., Storebakken, T., & Cui, Y. (1997). Effect of starvation on some morphological and biochemical parameters in white sturgeon, *Acipenser transmontanus*. Aquaculture, 151 (1-4), 357-363. https:// doi.org/10.1016/s0044-8486(96)01506-2

Jack, D.L., & Turner, M.W. (2003). Anti-microbial activities of mannose-binding lectin. Biochemical Society Transactions, 4, 753-757.

Jobling, M. (1980). Effects of starvation on proximate chemical composition and energy utilization of plaice, *Pleuronectes platessa* L. Journal of Fish Biology, 17(3), 325-334.

Jones, P., Binns, D., Chang, H.Y., Fraser, M., ..., & Hunter, S. (2014). InterProScan 5: genome-scale protein function classification. Bioinformatics, 30(9), 1236-1240. https:// doi.org/10.1093/bioinformatics/btu031

Jordan, S., Tung, N., Casanova-Acebes, M., Chang, C., ..., & Merad, M. (2019). Dietary intake regulates the circulating inflammatory monocyte pool. Cell, 178(5), 1102-1114. https:// doi.org/10.1016/j.cell.2019.07.050

Kaneko, G., Shirakami, H., Yamada, T., Ide, S., Haga, Y., Satoh, S., & Ushio, H. (2016). Short-term fasting increases skeletal muscle lipid content in association with enhanced mRNA levels of lipoprotein lipase 1 in lean juvenile res seabream (*Pagrus major*). Aquaculture, 452, 160-168. https://doi.org/10.1016/j.aquaculture.2015.10.030

Kutty, M.N. (1978). Ammonia Quotient in Sockeye Salmon (*Oncorhynchus nerka*). Journal of the Fisheries Research Board of Canada, 35(7), 1003-1005.

Li, B., & Dewey, C.N. (2011). RSEM: accurate transcript quantification from RNA-Seq data with or without a reference genome. BMC Bioinformatics, 12, 323.

Li, Q., Deng, L., & Diao, X. (2014). The effects of fasting on cortisol, metabolism of glucose in juveniles of *Pelteobagrus vachelli*. Freshwater Fisheries, 44 (1), 36-40.

Livak, K.J., & Schmittgen, T.D. (2001). Analysis of relative gene expression data using real-time quantitative PCR and the $2^{-\Delta\Delta CT}$ method. Methods, 25, 402-408.

Lu, D.L., Ma, Q., Wang, J., Li, L.Y., ..., Du, Z.Y. (2019). Fasting enhances cold resistance in fish through stimulating lipid catabolism and autophagy. Journal of Physiology, 597(6), 1585-1603. https:// doi.org/10.1113/jp277091

Lv, H., Hu, W., Xiong, S., You, J., & Fan, Q. (2018). Depuration and starvation improve flesh quality of grass carp (*Ctenopharyngodon idella*). Aquaculture Research, 49, 3196-3206. https:// doi.org/10.1111/are.13784

Mccue, M.D. (2010). Starvation physiology: reviewing the different strategies animals use to survive a common challenge. Comparative Biochemistry and Physiology, Part A, 156, 1-18.

Moon, Y.M., Lee, S.Y., Kwok, S.K., Lee, S.H., ..., & Cho, M.L. (2017). The Fos-related antigen 1–JUNB/Activator protein 1 transcription complex, a downstream target of signal transducer and activator of transcription 3, induces T helper 17 differentiation and promotes experimental autoimmune arthritis. Frontiers in Immunology, 8, 1793. https://doi.org/10.3389/fimmu.2017.01793

Morimoto, R.I., Sarge, K.D., & Abravaya, K. (1992). Transcriptional regulation of heat shock genes. A paradigm for inducible genomic responses. Journal of Biological Chemistry, 267, 21987-21990.

Ostojic, S.M., & Jorga, J. (2023). Guanidinoacetic acid in human nutrition: beyond creatine synthesis. Food Science & Nutrition, 11 (4), 1606-1611.

Park, C.J., & Seo, Y.S. (2015). Heat shock proteins: a review of the molecular chaperones for plant immunity. Plant Pathology Journal, 31, 323-333.

Poplawski, M.M., Mastaitis, J.W., Yang, X.J., & Mobbs, C.V. (2010). Hypothalamic responses to fasting indicate metabolic reprogramming away from glycolysis toward lipid oxidation. Endocrinology, 151(11), 5206-5217. https:// doi.org/10.1210/en.2010-0702

Qian, B., Xue, L., & Huang, H. (2016). Liver transcriptome analysis of the large yellow croaker (*Larimichthys crocea*) during fasting by using RNA-seq. Plos One, 11 (3), e0150240.

Rabinowitz, J.D., & White, E. (2010). Autophagy and metabolism. Science, 330(6009), 1344-1348.

Secor, S.M., & Carey, H.V. (2016). Integrative Physiology of Fasting. Comprehensive Physiology, 6(2), 773-825.

Wang, Z., Sun, B., & Zhu, F. (2018). Molecular characterization of glutaminyl-peptide cyclotransferase (QPCT) in *Scylla paramamosain* and its role in *Vibrio alginolyticus* and white spot syndrome virus (WSSV) infection. Fish & Shellfish Immunology, 78, 299-309. https://doi.org/10.1016/j.fsi.2018.04.059

Wu, Y., Liang, Z., Yuan, X., Chen, X., Liu, L., Li, X., & Li, C. (2011). Analysis and evaluation of nutritional components in the muscle of *Parabotia fasciata* Dabry. Freshwater Fisheries, 41 (1), 87-91. (In Chinese with English abstract)

Xie, C., Mao, X., Huang, J., Ding, Y., Wu, J., Dong, S., Kong, L., Gao, G., Li, C., & Wei, L. (2011). KOBAS 2.0: a web server for annotation and identification of enriched pathways and diseases. Nucleic Acids Research, 39, W316-322.

Xu, H., Jiang, Y., Miao, X.M., Tao, Y.X., Xie, L., & Li, Y. (2021). A model construction of starvation induces hepatic steatosis and transcriptome analysis in zebrafish larvae. Biology, 10(2), 92. https://doi.org/10.3390/biology10020092

Table S1. Statistics of sequencing and assembly results

Length Range	Transcript	Unigenes
200-300	20233(12.18%)	14 952(23.28%)
300-500	23490(14.14%)	13 257(20.64%)
500-1000	28548(17.19%)	13 219(20.58%)
1000-2000	31590(19.02%)	8 466(13.18%)
2000+	62224(37.47%)	14 332(22.31%)
Total Number	166085	64 226
Total Length	336364 015	90 668 740
N50 Length	3585	3 265
Mean Length	2025.25	1 411.71

Table S2. Summary of functional annotation result of *P. fasciata*

Item	Database									Total
	NR	Swiss-Prot	COG	GO	KOG	KEGG	Egg NOG	Pfam	TrEMBL	
Number	29 073	15 105	6 485	25 822	18 867	24 623	24 568	22 656	29 402	32 581
Percentage	89.23	46.36	19.9	79.43	57.9	75.57	75.41	69.54	90.24	100

Table S3. Statistics of annotated DEGs

|	COG	GO	KEGG	KOG	NR	Pfam	Swiss-Prot	eggNOG	Total
0 vs A3	70	330	324	213	373	299	235	312	375
0 vs A9	424	1358	1321	1055	1505	1282	906	1362	1513
0 vs A15	511	1754	1703	1347	1944	1706	1213	1721	1957
0 vs B3	155	550	537	413	602	526	405	538	605
0 vs B9	784	2068	1998	1652	2247	1964	1399	2053	2256
0 vs B15	294	899	875	681	1011	875	652	904	1018
0 vs C3	1219	3519	3431	2914	3781	3359	2390	3454	3800
0 vs C9	1176	3453	3364	2743	3762	3279	2397	3440	3781
0 vs C15	1057	2846	2783	2316	3088	2720	1989	2823	3101
A15vs B15	58	242	250	161	297	251	172	255	299
A15vs C15	284	819	809	636	916	771	584	817	922
A3 vs A15	619	1778	1748	1385	1968	1737	1218	1787	1981
A3 vs A9	679	2077	2022	1641	2276	1969	1399	2074	2288
A3 vs B3	198	544	525	422	591	498	368	548	591
A3 vs C3	1375	3950	3838	3189	4257	3772	2615	3880	4266
A9 vs A15	407	1528	1509	1156	1699	1467	1087	1521	1703
A9 vs B9	273	713	707	555	784	648	473	713	786
A9 vs C9	726	2011	1993	1564	2167	1912	1393	2012	2175
B15vs C15	322	763	754	610	832	717	536	760	835
B3 vs B15	104	402	403	301	468	373	294	411	473
B3 vs B9	616	1713	1655	1356	1871	1628	1137	1711	1879
B3 vs C3	749	1949	1904	1607	2086	1872	1271	1903	2093
B9 vs B15	313	1013	990	780	1118	959	688	1042	1126
B9 vs C9	244	672	673	535	747	619	468	679	753
C3 vs C15	380	1327	1311	1002	1492	1253	913	1341	1496
C3 vs C9	1001	3220	3142	2578	3563	3081	2184	3209	3574
C9 vs C15	321	1003	1000	768	1151	955	667	1011	1158
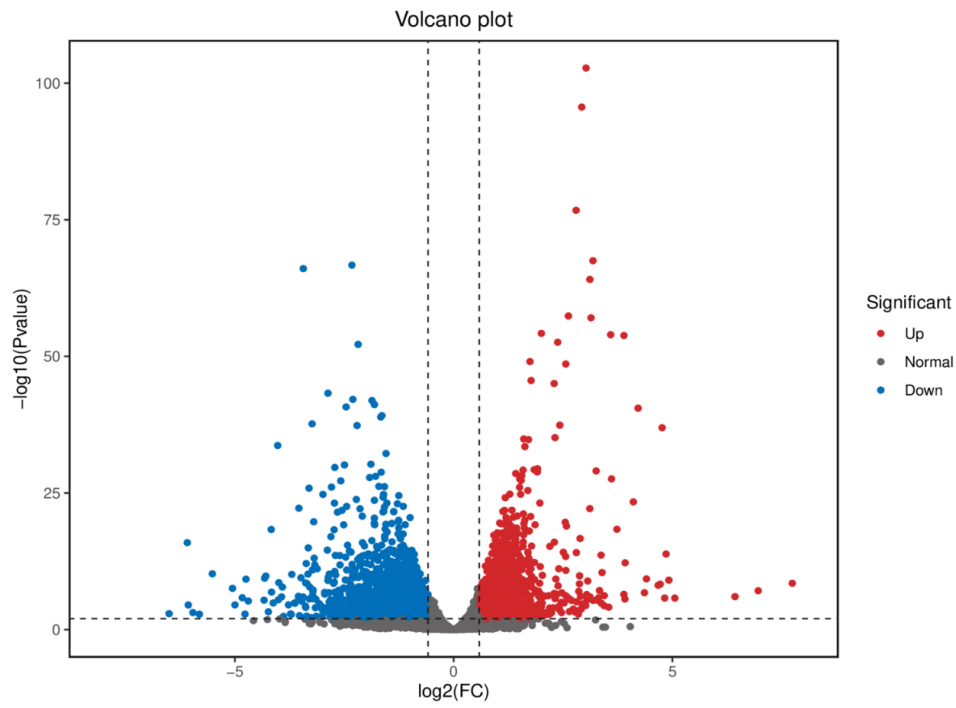
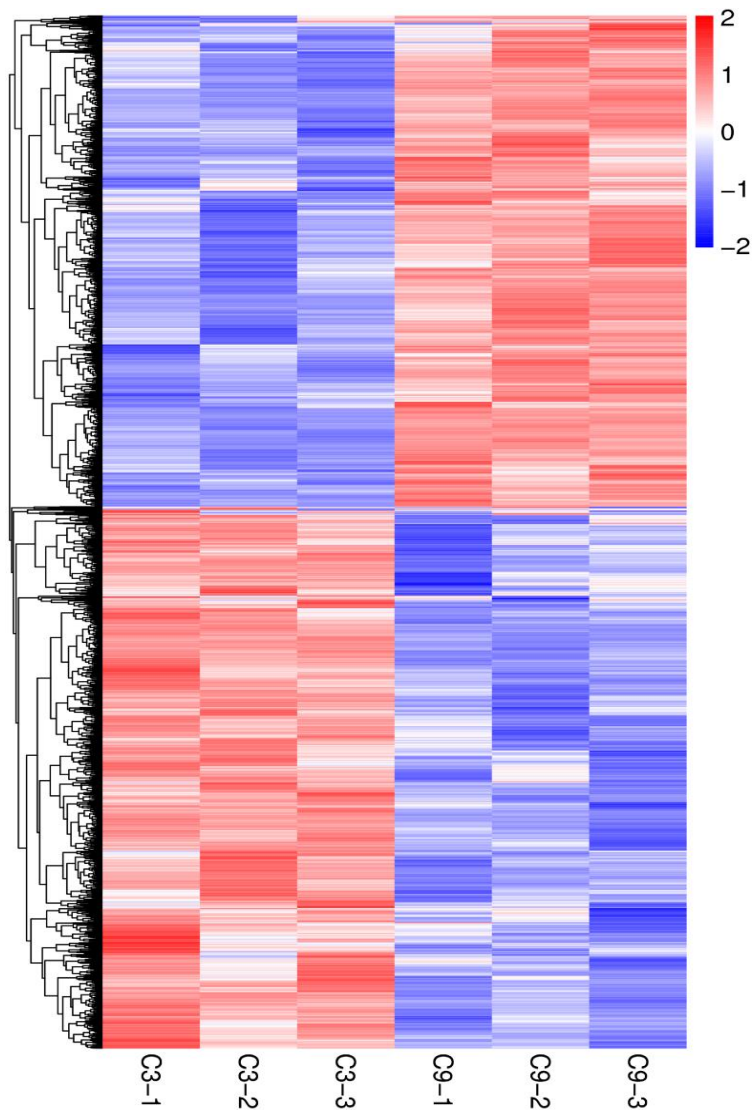**Figure S1.** Volcano plot of DEGs between groups C3 and C9

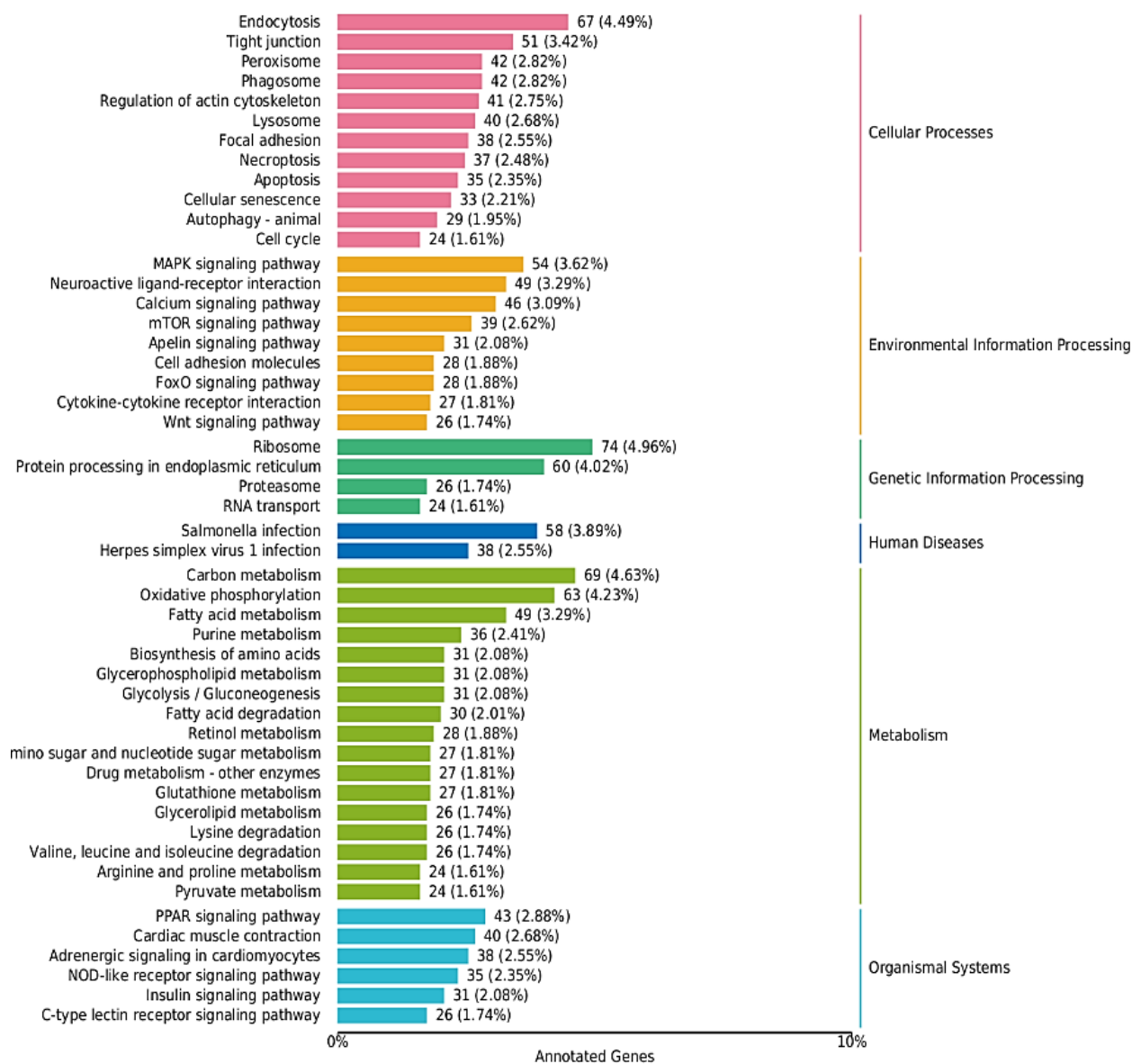**Figure S2.** Heatmap of clustered differential gene expression between C3 and C9.
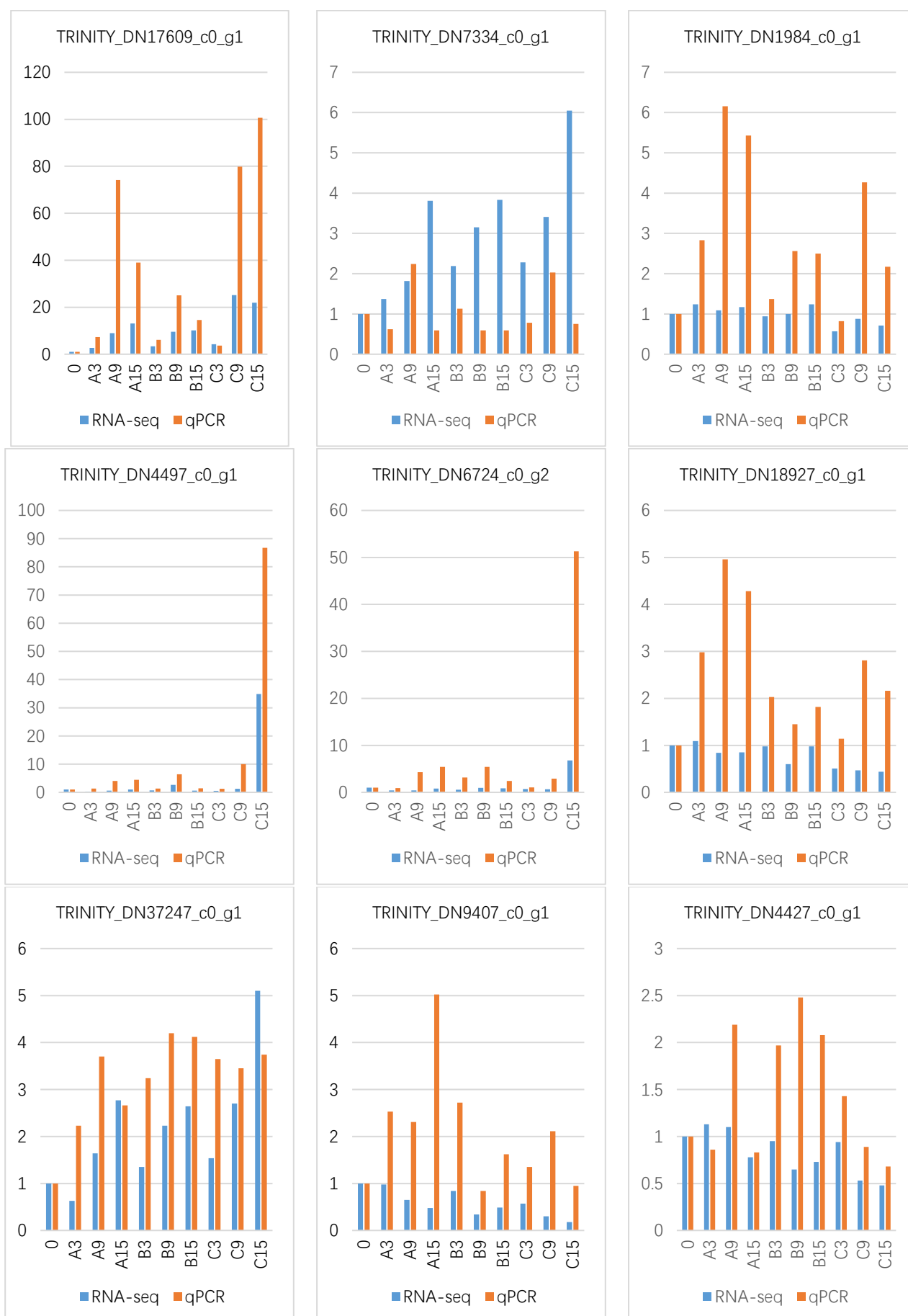
Figure S3. KEGG enrichment pathways

Figure S4. Comparison of relative fold change between RNA-seq and qPCR results